Proc. Natl. Acad. Sci. USA
Vol. 86, pp. 4397–4401, June 1989
Biochemistry

tRNA–tRNA interactions within cellular ribosomes

(context effect/RNA structure/translation/suppressor)

DREW SMITH* AND MICHAEL YARUS†

Department of Molecular, Cellular, and Developmental Biology, University of Colorado, Boulder, CO 80309-0347

Communicated by Paul Berg, March 16, 1989

ABSTRACT **We describe an assay that converts the effects of tRNA–tRNA contacts at two particular codons into a quantitative effect on β-galactosidase level. The assay measures the separate and combined efficiency of suppression at adjacent nonsense codons *in vivo* using a set of specially created homologous messages. In a survey of distal anticodon arm substitutions, we find that particular mutant tRNAs occupying the P-site reduce the apparent efficiency of the suppressor tRNA reading the A-site codon by factors of 2–170. By using measured tRNA–tRNA distances and the crystallographic tRNA structure, we propose a model of the tRNA–tRNA–mRNA complex. In the model, the anticodon loops of the P-site and A-site tRNAs contact one another in a way that is consistent with our combined tRNA efficiency data. These results suggest that tRNA–tRNA interactions that modulate tRNA action are an inevitable feature of translation.**

There are several reasons to suspect that tRNAs interact with one another on the ribosome. One reason, perhaps the most compelling, is found in the topology of translation: tRNAs bind adjacent codons, and nascent peptide must be transferred to the incoming amino acid. Thus both the anticodon loops and 3′ ends of the P-site and A-site tRNAs should approach one another at some time, if not throughout the translational cycle. This reasoning finds experimental support in the measurement of the distances between fluorescent probes attached to ribosome-bound tRNAs (1–3), which places A- and P-site tRNAs no more than a few angstroms apart.

The non-uniform nature of the translational process suggests that tRNA–tRNA interactions have a functional significance: the rate at which a codon is read appears not to be constant but depends on the identity of the codon's neighbors, a phenomenon known as the "context effect" (4–7). Contacts between tRNAs have been proposed as one source of non-uniformity (4, 8): different sets of contacts for different pairs of A- and P-site tRNAs alter the rate of A-site occupation.

We have designed a genetic assay for functionally significant tRNA–tRNA interactions that appreciably alter the rate of aminoacyl-tRNA selection. The principle of this assay can best be described by its null hypothesis: if tRNAs do not interact, then translation of a codon should be insensitive to changes in the structures of neighboring tRNAs. A test of the hypothesis requires a system in which translation at a specified codon can be monitored when the structure of a neighboring tRNA is altered.

Fig. 1 outlines such a system. The plan of the experiment is to alter a single site in the P-site tRNA and to measure the rate of aminoacyl-tRNA selection at the adjacent codon as compared to a control. The tRNAs translating both codons can be controlled, and translation at the A-site codon can be measured during the steady state *in vivo* by using nonsense suppressor tRNAs. The probability of suppression measures the rate at which the A-site tRNA translates its codon (9, 10), because a nonsense suppressor tRNA competes with its release factor. We vary the UAG suppressor tRNA at the P-site and use a constant UGG/UGA-reading tRNA for the other codon. During translation of both controls and the test message (Fig. 1), both ribosomal sites are occupied by a derivative of $tRNA^{Trp}$ (*E. coli*). Thus tRNA–tRNA interfaces are equivalent throughout the experiment except for the effects of a single change in the P-site tRNA.

The null hypothesis of no interaction posits that translation of neighboring codons is independent. For nonsense suppression this means that the probability of transmission of the nascent peptide (rather than termination), also called the efficiency of suppression, of adjacent codons is independent. Experimentally, if suppression efficiency in the test allele with adjacent nonsense codons (Fig. 1 *Right*) differs significantly from the product of the efficiencies of the controls having single nonsense codons (Fig. 1 *Left*), this difference reflects the effect of the structural alteration of the UAG (P-site) suppressor acting on the efficiency of the UGA (A-site) suppressor. We call the ratio of the observed to expected efficiency the translational nonindependence. This ratio increases as interference between tRNAs increases.

The source of the signal in this assay needs special emphasis. Since the mutant P-site tRNA has an A-site neighbor in both control and test, one might expect the potential effects of a P-site mutation to manifest themselves in both the control and the test (Fig. 1). How, then, is translational nonindependence detected? The answer is that reduction in the rate of A-site occupancy by a sense tRNA at a sense codon (in the control) slows transit of 1 codon in 1028 along the *lacZ* message, with small or no effect on the gene product. A similar reduction in the rate of A-site occupation by a nonsense suppressor tRNA at a nonsense codon (in the test), however, can increase the probability of termination by release factor and so cause a marked reduction in the yield of gene product. Our test exploits the difference between sense and nonsense codons to amplify rate differences in tRNA selection as a result of changes in a single tRNA–tRNA interface.

By using this system, we have identified tRNA structures that affect the efficiency of translation at adjacent codons and, by use of a second test, distinguished direct effects (i.e., those attributable to tRNA–tRNA contacts) from indirect interactions.

RESULTS

tRNA–tRNA Interactions Can be Detected by Genetic Means. The results of the survey of P-site tRNA structures that can affect translation at the A-site are shown in Fig. 2, which plots the expected/observed suppression at UAG

The publication costs of this article were defrayed in part by page charge payment. This article must therefore be hereby marked "*advertisement*" in accordance with 18 U.S.C. §1734 solely to indicate this fact.

*Present address: Department of Biology, Indiana University, Bloomington, IN 47405.
†To whom reprint requests should be addressed.

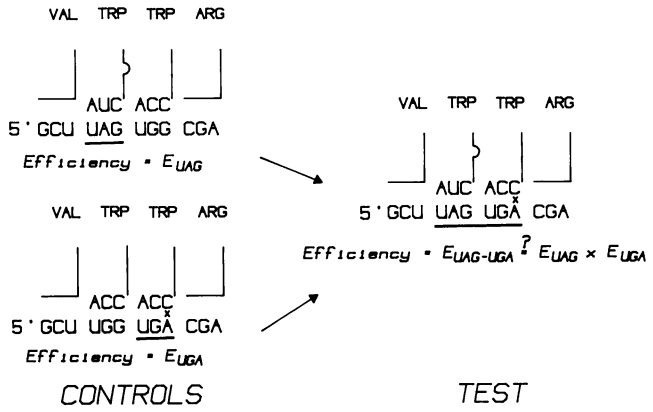

FIG. 1. Test for functional tRNA–tRNA interactions. tRNAs are shown binding to their codons in the two control (*Left*) and test (*Right*) messages. If tRNAs do not interact, or their interactions are equivalent, suppression efficiency of the test message ($E_{UAG-UGA}$) should equal the product of the efficiencies of the controls ($E_{UAG} \times E_{UGA}$). Amino acid abbreviations denote parental tRNAs; UAG suppressor derivatives of $tRNA^{Trp}$ actually insert gluatmine. Termination codons, whose tRNAs are manipulated in these tests, are underlined. The strains used are *Escherichia coli* K-12 (*Δlac–pro, recA56, trpT178*). The UGG/UGA-translating tRNA (Su9 ≡ Su7 A24) replaces $tRNA^{Trp}$ on the chromosome, the *lacZ* alleles are carried on a chloramphenicol-resistant plasmid with a p15a origin (9), and the UAG suppressor tRNA gene is carried on a compatible colE1 origin, tetracycline-resistant plasmid (10). Strains were grown and β-galactosidase activity was assayed as described (9).

UGA against the expected suppression. Translational nonindependence is indicated by distance along the *y* axis; the *x* axis is not the independent variable but serves to separate the UAG suppressor tRNAs in order of increasing activity (Fig. 2 legend). The tRNAs used are a set of site-directed mutant derivatives of the *E. coli* $tRNA^{Trp}$-based UAG suppressor Su7 (10, 11), which saturate the anticodon loop and distal portion of the anticodon stem. We begin with a discussion of the controls built into this assay and of the nature of the information provided by it.

Suppression Efficiency and Nonindependence Are Unconnected. Since the *x* axis orders the UAG suppressors by their activity, the graph in Fig. 2 shows what, if any, relationship exists between suppression efficiency (the fraction of nascent peptides transmitted) and nonindependence in the translation of adjacent codons. Nontranslational or indirectly translational effects, such as transcriptional polarity, might reveal themselves through a dependence on suppression efficiency. For polarity, the points should fall on a line with a negative slope: nonindependence should decrease as suppression efficiency increases. Although there may be a trend in this direction, the data show that there is no necessary relationship between suppression efficiency and translational nonindependence, as weak suppressors often show no more nonindependence than the parental suppressor Su7 or other efficient suppressors. In addition, suppressors of similar efficiency often show different levels of nonindependence.

Effects of Cell Physiology on Nonindependence Are Controlled. The argument that nonindependence is a directly translational property is supported by a survey of mRNA levels of the reporter *lacZ* alleles in a sample of tRNA mutant strains (Su7, A32, A33). RNA from the appropriate strains, which show the extreme of nonindependence we have observed (Fig. 2), was extracted and immobilized on Amersham Hybond-N filters by use of a dot-blot manifold. The RNA was probed (9) by ^{32}P-labeled synthetic oligonucleotides complementary to the 5′ or 3′ ends of the *lacZ* coding sequence. Differences in the levels of mRNA from the test and control alleles were never found to vary by more than a factor of 3,

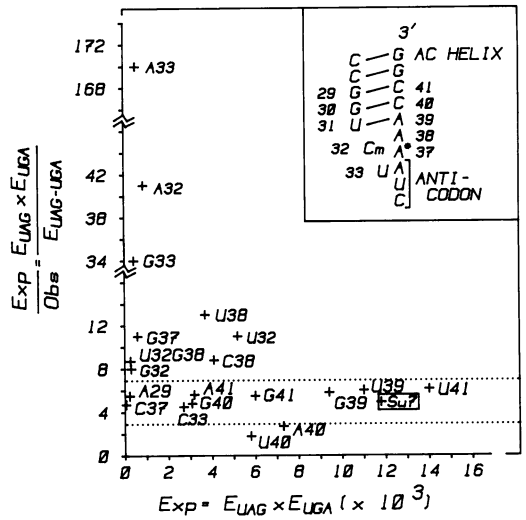

FIG. 2. Effect of P-site tRNA anticodon arm mutations on tRNA–tRNA interactions. The *x* axis plots suppression efficiency expected (Exp) at UAG UGA if tRNAs do not interact: $E_{UAG} \times E_{UGA}$. E_{UGA} is nearly constant, 1–2%, and thus the mutant UAG suppressors are ordered by their efficiency, most efficient on the right. The *y* axis plots the ratio of suppression efficiency expected at UAG UGA ($E_{UAG} \times E_{UGA}$) to that actually observed (Obs) ($E_{UAG-UGA}$). If $E_{UAG} \times E_{UGA}/E_{UAG-UGA}$ is >> 1, the mutation in the P-site tRNA is reducing suppression efficiency at the A-site. No suppression of the UAG UGA test allele was detectable for A33 and G37: the ratios shown are minimal. The homologous pseudo-wild allele produces 15,800 units of β-galactosidase activity. Helix mutations are named by their 3′ member (positions 39, 40, 41) when the complementary second mutation is implied. A29, an A29–C41 mismatch, is the single deviation. Standard errors are *ca.* 20% of the values on each axis. The parental Su7 suppressor is boxed, and a band representing ±2 standard errors (dotted lines) is centered on the Su7 point. (*Inset*) tRNA anticodon arm, showing the parental Su7 sequence and the numbering for mutations. A* = ms^2i^6A.

a difference that is insufficient to account for the observed translational nonindependence.

Potential physiological effects of the two termination suppressors cannot account for translational nonindependence. All measurements for one tRNA are made in isogenic strains with both suppressors present in both controls and test. The bacteria are therefore genetically and physiologically identical. The sole differences between the control and test strains are the single nucleotide substitutions in the reporter gene (*lacZ*, Fig. 1), which is not required for cell growth.

Comparison of tRNA's Controls for mRNA Structure. The ratio of expected to observed suppression at adjacent codons could reflect not only tRNA–tRNA interactions but also two differences in the control and test mRNAs found at the second position of the P-site codon and in the third position of the A-site codon (Fig. 1). These mRNA sequence differences may contribute, through effects on mRNA levels or structure, a basal difference between control and test efficiencies. This effect may perhaps be observed in the example of Su7, which differs minimally from normal $tRNA^{Trp}$, having the same sequence outside the anticodon. The expected/observed value for Su7 (Fig. 2) indicates that translation at the adjacent nonsense codons is five times less efficient than expected.

Therefore, our analysis compares nonindependence for different tRNAs to one another rather than to theoretical values. Because all tRNAs translate the same messages, any effects of the messages on nonindependence are systematic. Thus we conclude, for instance, that the introduction of the A33 mutation into the P-site tRNA causes a 30-fold increase in translational nonindependence (compare Su7 A33 to Su7).

tRNA Structure and Nonindependence. The anticodon loop is more influential than the helix in determining nonindependence. Fig. 2 shows that 9 of 20 of the anticodon helix and loop substitutions tested significantly increase translational nonindependence above the level observed for the minimally altered suppressor, Su7. Increases in nonindependence are observed at all four of the mutated positions in the anticodon loop. Of the 11 loop substitutions tested, only 2 (C37 and C33) fail to appreciably increase nonindependence. Notably, loop substitutions that alter nonindependence always *increase* it: the wild-type anticodon loop in Su7 appears optimal for the adjacent tRNA.

In contrast, 0 of 9 base-pair substitutions at three positions in the stem increase nonindependence over the basal level, and 2 (A40 and U40) cause a slight reduction. The stem therefore is a minor site of tRNA–tRNA interaction; even the mid-helix mispair mutant (A29-C41) has no appreciable effect on nonindependence.

The 5′ Side of the Anticodon Loop Is Most Influential. P-site tRNAs with purine substitutions in the 5′ side of the anticodon loop (positions 32 and 33) show the most marked interactions, decreasing A-site suppression efficiency >30-fold below the level of the unmutated suppressor. The effect at position 33 is greater than the effect at position 32, and the substitution of adenine has a larger effect than the substitution of guanine at both positions. Because pyrimidine substitutions here show smaller effects (especially C33), it is likely that the greater size of the purine bases contributes to their high levels of nonindependence. We will argue that these purines on the P-site tRNA produce nonindependence in translation by occlusion of the A-site.

Substitutions on the 3′ side of the anticodon loop (positions 37 and 38) have smaller effects on nonindependence. These substitutions may cause an ≈2-fold increase in nonindependence relative to the parental suppressor (Su7), but we see no clear pattern that relates nonindependence to position or type of substitution. The effects of these mutations may be communicated through loop structure rather than through immediate contacts of the mutated base with the A-site tRNA. Comparison of the nonadditivities of the U32 tRNA with that of the double mutant U32G38 supports this interpretation. Introduction of the G38 mutation somewhat reduces the nonadditive effects of the U32 mutation, and positions 32 and 38 oppose each other across the anticodon loop (Fig. 2 *Inset*), where an interaction between them is quite plausible.

A Test for Specific Contacts Between tRNAs. Although these experiments detect significant interactions between tRNAs, they do not distinguish direct structural contacts of the mutated base from those that have a more indirect mechanism. One test of direct interactions is to determine the dependence of the effects on the relative orientation of the two tRNAs. A mutant base in the P-site (UAG suppressor) tRNA that contacts the A-site (UGA suppressor) tRNA cannot make the same contact when the tRNAs are exchanged. An indirect effect (e.g., through suppression of natural terminators) would have a similar effect on nonindependence regardless of the tRNA–tRNA interface in our test message. We repeated our measurements using a set of *lacZ* messages in which codon order has been reversed; UGA is the P-site codon and UAG is the A-site codon.

Fig. 3 shows that most of the nonindependence has disappeared upon reversal of codon order, most notably for tRNAs with substitutions on the 5′ side of the anticodon loop (A33, A32, U32). Whereas these substitutions lowered suppression by a factor of 10–170 below that expected in the codon order UAG UGA, this factor is reduced to 1–4 in the order UGA UAG and is not very different from the parental suppressor (Su7). Because nonindependence in translation caused by these tRNAs is very dependent on tRNA–tRNA orientation, they meet this criterion for direct interaction.

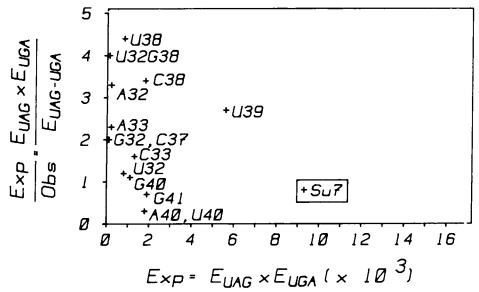

FIG. 3. Effect of relative orientation on tRNA–tRNA interactions: Nonindependence after reversal of codon order. See the legend to Fig. 2 for explanation of the axes.

DISCUSSION

The Case for tRNA–tRNA Contacts. The results we present in this paper show that changes in the structure of a tRNA at one codon affect translational efficiency at its 3′ neighboring codon. The highly controlled nature of the experiments with respect to cell physiology, mRNA levels, mRNA structure, and tRNA structure leads us to conclude that the defined mutations introduced into the suppressors are in fact the source of measured changes in translational nonindependence.

Though interaction through the ribosome is possible, we believe that the simplest explanation of the data is one of tRNA–tRNA interactions, either by contacts of two tRNAs mediated by the mutant bases or indirectly through contacts at a second site. Direct interactions define the area of contact and so are informative with respect to the topology of the tRNA–tRNA–mRNA complex on the ribosome. The indirect effects of substitutions (i.e., on the 3′ side of the loop) are less informative with respect to translational topology but also identify tRNA structures that affect formation of a productive ribosomal complex.

The 5′ Side of the P-Site Anticodon Loop Contacts the A-Site tRNA. The substitution of purines for the conserved pyrimidines in the 5′ side of the anticodon loop produces the greatest departure from expectation (≥170-fold), and this effect depends critically on the physical interface between the P- and A-site tRNAs (Figs. 2 and 3). The simplest interpretation of these results is that the 5′ side of the mutant P-site anticodon loop is in contact with the A-site tRNA at the site of the mutations. Substitution by the larger purine bases may actually occlude the A-site and so reduce the rate at which the A-site tRNA is accepted at the A-site codon. This may explain the virtually universal occurrence of pyrimidines at positions 32 and 33 in natural tRNAs.

Nature of the Contacts. There is a chemical effect of 5′ anticodon loop substitutions. At both positions 32 and 33, adenine has a greater negative effect than guanine. Because the molecular mass of adenine is less than that of guanine, size is not the sole factor in determining nonindependence: unfavorable tRNA–tRNA interactions are either ameliorated by the exocyclic groups of guanine (2-amino and 6-keto) or worsened by the exocyclic group of adenine (6-amino).

Another nonsteric effect may account for the phenotype of the U32 substitution, which causes as much nonindependence as G32. Note that the effect of this transition substitution is greater than that of the equivalent one at position 33 (C33, see Fig. 2). The phenotype of U32 may be related to its effects on 2′ O-methylation of ribose 32: U32 reduces methylation more than any other of the loop substitutions (10). Possibly this methyl group is involved in a favorable tRNA–tRNA contact, and so its loss is equivalent to interference.

A Model of the tRNA–tRNA–mRNA Complex. We wish to show that our genetic test leads to a plausible molecular complex. The following structural discussion refers to the

rate-limiting steps during binding of a new aminoacyl-tRNA, which is when the outcome of our experiment is determined.

Beginning with A- and P-site tRNAs in the conformation of yeast $tRNA^{Phe}$ (12), we arranged the molecules to conform with the measurement of the distances between fluorescent bases on ribosome-bound tRNAs (1–3), with the additional constraint that the 3′ ends (which bear the peptide and the amino acid) be within 25 Å of one another. The flexibility of the 3′ extension can easily be used to bring the 3′ ends together from this distance. All of these constraints cannot be accommodated simultaneously without some overlap of the van der Waals' radii of the two tRNAs. The final model is outside of the reported experimental error for one of the five distance measurements.

Next we adjusted the model to permit contacts suggested by the genetic data and paired a two-codon segment of helical RNA to both anticodons. At this stage, close contacts between the anticodon wobble nucleotide of the P-site tRNA and the hypermodified purine 37 of the A-site tRNA appeared. Such close contacts are nearly inevitable at the junction between the P- and A-site anticodons, which must be brought together to pair with a continuous message. These contacts were relieved using *ca.* 20° rotation of the P—O3′ bonds flanking A-site nucleotide 37, well within the range observed for P—O3′ bonds in oligonucleotides and tRNA itself (12). Perhaps the frequent modification of nucleotide 37, just 3′ to the anticodon (Fig. 2 *Inset*), facilitates this tRNA–tRNA contact. Our final model (see Fig. 5) suggests that message can plausibly contact both anticodons while the tRNAs interact as required to satisfy the genetics.

Synthesis of Genetic and Crystallographic Data. The general form of this model (Fig. 4) is roughly similar to that originally proposed by Rich (13): near approach of the anticodon regions and 3′ ends and an angle between the planes of the tRNAs. The gap between the 3′ base of the P-site codon and the 5′ base of the A-site codon is 10 Å, a distance that sets the helices of the anticodon stems in register and so reduces potential hindrance between them. The closest approach of the two tRNAs is at their anticodon loops. However, the variable loop of the P-site tRNA approaches the D-loop of the A-site tRNA, suggesting that these regions could be involved in tRNA–tRNA interactions. We propose that the trans-dominant mutations in the variable loop of $tRNA^{Phe}$, reported to deattenuate the PheRS operon (14), may be defective in tRNA–tRNA interactions in this region.

Fig. 5 focuses on the anticodon loops. Our genetic results show a functional interaction of the 5′ side of the P-site tRNA anticodon loop with the A-site tRNA. The model allows the most influential bases of the P-site loop (32 and, particularly, 33) to approach the A-site tRNA at bases 38–40, just 3′ to its anticodon. We therefore predict that mutations in the A-site tRNA at nucleotides 38–40 will alter and perhaps revert the nonindependence caused by purine 32 and 33 substitutions.

In Fig. 5, A33 is in the syn conformation permissible for purines. This transformation allows the base to be better accommodated within an anticodon loop of normal conformation. The syn conformation is also suggested by our genetic data, because adenine produces more interference than guanine at both positions 32 and 33. The data thus suggest the participation of the exocyclic groups in the tRNA–tRNA contacts, and these groups are not readily available to the A-site tRNA unless the bases at position 33 of the P-site tRNA are rotated to the syn conformation. In this model, the van der Waals' radius of the P-site tRNA A33-amino overlaps the backbone at nucleotides 38–39 of the A-site tRNA, producing a partial occlusion of the A-site.

The difference between the unmutated anticodon loop and the A33 loop is small and requires extremely close approach of the loops for A33 in the P-site to contact the A-site tRNA. The distance that A33 (syn) protrudes is at most only 2.3 Å more than U33. Therefore 2.3 Å is an estimate of the *maximal* distance between unperturbed nonmutant anticodon loops at this point. This small distance allows the tRNAs to interact via hydrogen bonding and electrostatic and London forces. Indeed, such interactions are unavoidable at this distance.

Comparison with Previous Models. It is difficult to reconcile these results with models in which ribosome-bound tRNAs are not side by side; for example, Woese's reciprocating rachet (15). Even in previous side-by-side models (3, 13, 16–18), the 5′ side of the P-site loop does not seem to contact the A-site tRNA. Therefore, the disposition of the tRNAs in Figs. 4 and 5 is novel in this respect. Put another way, it now seems fair to conclude that the P-site tRNA anticodon loop forms one wall of the A- or coding site within the ribosome.

Implications for RNA Structure. It seems plausible that the anticodon loops of tRNAs have evolved to make their contacts in the A- and P-sites favorable, given that contact between anticodon loops is expected to be destabilized by electrostatic repulsion between the negatively charged phosphates of the tRNA backbones. The near-universal conservation of pyrimidines on the 5′ side of anticodon loops may be one expression of this constraint (see Fig. 2).

In our model, several plausible hydrogen bonds can be drawn between 2′-OH groups on one tRNA and phosphate

FIG. 4. Model for the tRNA–tRNA–mRNA complex on the ribosome. The P-site tRNA (in cross-eyed stereo) is on the left and the A-site is on the right. The tRNA 3′ ends are at the top. The portion of the tRNA varied in these experiments is shown in detail, and the rest of the tRNA is represented as a line connecting phosphates.

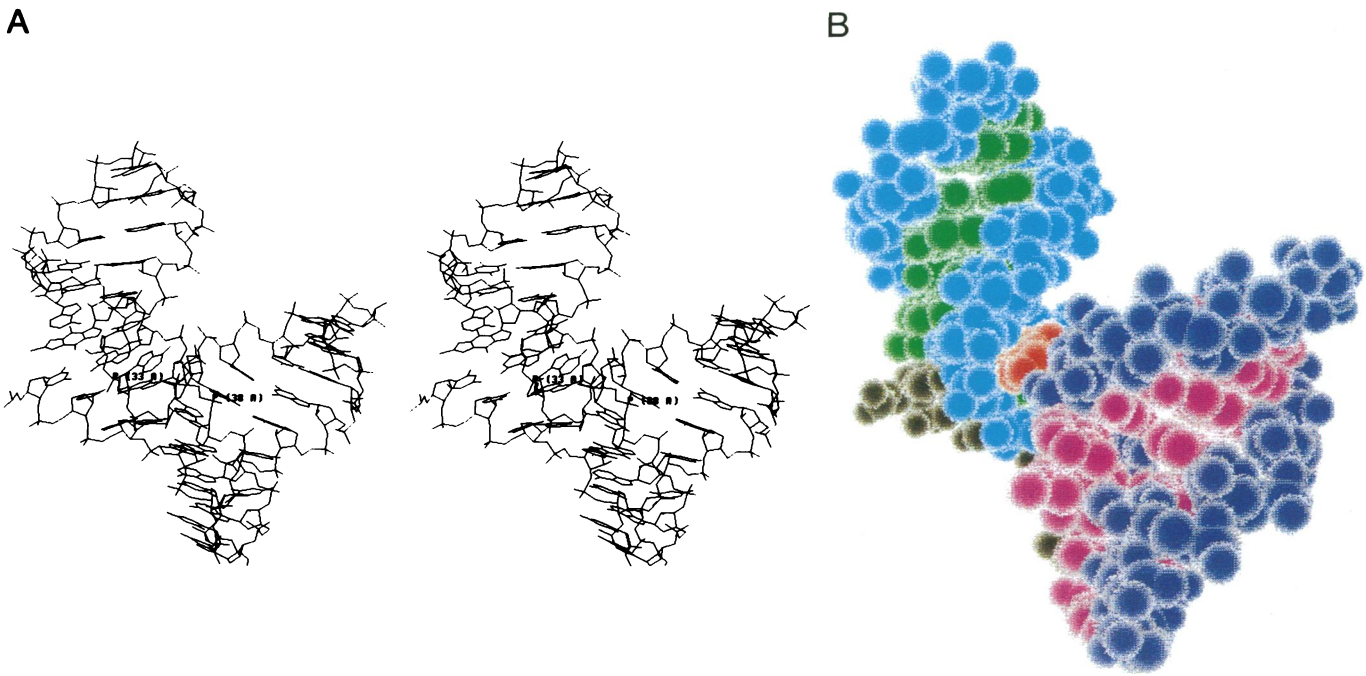

FIG. 5. Close-up of anticodon arms and message, in the same orientation as Fig. 4. (*A*) Adenine has been substituted for uracil at position 33 in the P-site tRNA. The rotation of the base to the syn conformation causes it to protrude into the groove behind the P-site tRNA anticodon. (*B*) Space-filling model. RNA backbones are shown in light and dark blue on the P- and A-site tRNAs, respectively; the bases are green and magenta, respectively. The base moiety of A33 is red-orange. The black structure most clearly visible at left is the message.

oxygens and 3-O groups on the other. A slight unwinding of the A-site anticodon stem would allow others, including uridine-2′-OH bonds like those described for an RNA crystal (19). This tRNA–tRNA complex is an intermolecular nonhelical RNA–RNA interaction that may have found other uses. We note that the loops involved in the initial binding of the colE1 origin RNA I and primer to one another have structures that mimic anticodon loops (20).

tRNA–tRNA Interactions and Gene Expression. We believe that tRNA–tRNA interactions of the type we have described apply to the mechanics of the normal translational cycle. Although many of our mutations create unnatural tRNA sequences (e.g., A33), others are common (e.g., U38) to wild-type tRNAs and so are likely to exemplify the effects of sequence differences between wild-type tRNAs. In experiments not shown, we compared a series of amber suppressors that differ from normal parental tRNAs only in their anticodons (e.g., ref. 21). We find a 9-fold range of nonindependence for these tRNAs. This further supports the notion that tRNA–tRNA interactions differ among normal tRNAs. This should alter translational step time and ultimately gene expression.

This conclusion is also consistent with that of Yarus and Folley (7), who noted a pattern of correlation between the identities of the third nucleotides of adjacent codons in weakly expressed *E. coli* genes. They suggested that this spacing precludes a direct effect of the correlated bases on each other or on the adjacent tRNA and may instead require contact between adjacent tRNAs. It was subsequently shown (8) that introduction of this pattern into a message can reduce gene expression.

These experiments were supported by National Institutes of Health research Grant GM30881 to M.Y.

1. Fairclough, R. H. & Cantor, C. R. (1979) *J. Mol. Biol.* **132,** 575–586.
2. Johnson, A. E., Adkins, H. J., Matthews, E. A. & Cantor, C. R. (1982) *J. Mol. Biol.* **156,** 113–140.
3. Paulsen, H., Robertson, H. J. & Wintermeyer, W. (1983) *J. Mol. Biol.* **167,** 411–426.
4. Bossi, L. (1983) *J. Mol. Biol.* **164,** 73–87.
5. Miller, J. H. & Albertini, A. M. (1983) *J. Mol. Biol.* **164,** 59–71.
6. Murgola, E. J., Pagel, F. T. & Hijazi, K. A. (1984) *J. Mol. Biol.* **175,** 19–27.
7. Yarus, M. & Folley, L. F. (1985) *J. Mol. Biol.* **182,** 529–540.
8. Folley, L. S. & Yarus, M. (1989) *J. Mol. Biol.*, in press.
9. Smith, D. & Yarus, M. (1989) *J. Mol. Biol.* **206,** 489–501.
10. Yarus, M., Cline, S. W., Wier, P., Bradley, D., Breeden, L. & Thompson, R. C. (1986) *J. Mol. Biol.* **192,** 235–255.
11. Yarus, M. (1982) *Science* **218,** 646–652.
12. Holbrook, S. R., Sussman, J. L., Warrant, R. W. & Kim, S.-H. (1978) *J. Mol. Biol.* **123,** 631–660.
13. Rich, A. (1974), in *Ribosomes*, ed. Nomura, M., Tissieres, A. & Lengyel, P. (Cold Spring Harbor Lab., Cold Spring Harbor, NY), pp. 871–885.
14. Vacher, J., Springer, M. & Buckingham, R. H. (1985) *EMBO J.* **4,** 509–514.
15. Woese, C. (1970) *Nature (London)* **226,** 817–820.
16. Sundaralingam, M., Brennan, T., Yathindra, N. & Ichikawa, T. (1975) in *Structure and Conformation of Nucleic Acids and Protein–Nucleic Acid Interactions*, eds. Sundaralingam, M. & Rao, S. T. (University Park, Baltimore), pp. 101–115.
17. Spirin, A. S. (1985) in *Progress in Nucleic Acid Research*, eds. Cohn, W. E. & Moldave, K. (Academic, New York), Vol. 32, pp. 74–114.
18. McDonald, J. J. & Rein, R. (1987) *J. Biomol. Struct. Dyn.* **4,** 729–744.
19. Dock-Bregeon, A. C., Chevrier, B., Prodjarny, A., Moras, D., deBear, J. S., Gough, G. R., Gilham, P. T. & Johnson, J. E. (1988) *Nature (London)* **335,** 375–378.
20. Lacatena, R. M. & Cesareni, G. (1983) *J. Mol. Biol.* **170,** 635–650.
21. Normanly, J., Masson, J.-M., Kleina, L. G., Abelson, J. & Miller, J. H. (1986) *Proc. Natl. Acad. Sci. USA* **83,** 6548–6552.